

A NOVEL METHODOLOGY FOR THE AUTOMATIC ACQUISITION OF REAL FOREST FIRE DATASETS OVER LONG PERIODS OF TIME

G. E. Suárez-Fernández^{1*}, J. Martínez-Sánchez¹, P. Arias¹

¹ Applied Geotechnologies Research Group, University of Vigo, ETSE Minas, 36310 Vigo (Spain) – (gabrieleduardo.suarez*, joaquin.martinez, parias)@uvigo.es

KEY WORDS: Forest Fire, Spatial Analysis, Image Processing, Landsat, Remote Sensing, Burned Areas, Mapping.

ABSTRACT:

Forest areas or green infrastructure have become a fundamental economic and social factor which has made it possible to generate new sources of employment and to maximize the use of basic resources. Nevertheless, good conservation of this type of infrastructure is a challenge. This is due to the problems deriving from, on the one hand, the increase of its physical scope and, on the other, poor management or no management at all. The Spanish region of Galicia is a historic place of natural wealth, especially concerning forest resources, wherein 2/3 of its territory is forest area from where more than half of the Spanish wood supply comes.

This paper seeks to create a mapping of major forest fire disturbances on the Galician territory over extended periods of time. To achieve this, an automated multitemporal detection process based on vegetation indices and unsupervised learning is developed. The objective is to obtain data heterogeneity in terms of vegetation state, land use, and image properties, allowing a better understanding of forest land disturbances and improving their management.

1. INTRODUCTION

Green infrastructure or forest areas have been a fundamental economic and social factor. The New Strategy of the European Union recognizes the multifunctional role of this type of infrastructure to achieve a fully green and carbon-neutral economy by 2050 (European Commission, 2021).

However, there is a risk associated with green infrastructure. Risk can be understood as (1) the hazard of a latent damaging event to the infrastructure, (2) the susceptibility of the elements and the environment, and (3) the values of the elements susceptible to loss (Jactel et al., 2012). The wildfires are a main risk related to forest, affecting both ecological preservation and the safety and proper development of people and countries (Haynes et al., 2020). As a result, it is necessary to characterize, classify and locate the decisive aspects that boost this type of pathologies.

The lack of an accurate inventory of forest fires with a broad time frame is one of the main problems to better understand these disturbances. Currently, there are platforms that make use of several sources of information to detect active fires and to determine their extent (European Forest Fire Information System (EFFIS); NASA EarthData Worldview). Nevertheless, the implementation of this type of platforms is recent.

Remote Sensing Technologies are used as a method to assess vegetation health (Yang et al., 2022), detect changes in land use (Das & Angadi, 2022), classify fuel types (Labenski et al., 2022), and detect perimeters and severity of forest fires (Ban et al., 2020; Jiao & Bo, 2022). The availability of satellite images is a valuable tool that enables mapping and identification of forest fire areas with different spatial, temporal, and spectral resolutions (Chuvieco et al., 2019). The medium spatial resolution satellite imagery has shown promise for detecting burned areas (Hawbaker et al., 2020; Loboda et al., 2013), allowing the

identification of smaller objects. In addition, the use of spectral indices based on certain electromagnetic spectrum bands has been widely used by different authors to determine the severity of wildfires (Cocke et al., 2005; Escuin et al., 2008; Mallinis et al., 2018).

The large availability of free multispectral images, mainly from the Landsat mission, which has a broad time frame, makes it possible to obtain multispectral images (RGB and Infrared spectrum) with medium spatial resolution for approximately the last 35 years. This wide range of data provides valuable information about the condition of the natural environment and disturbances occurring over various periods of time.

In this way, Spain is among the top five European countries with the highest number of forest fires and burned area (European Commission, 2022). These fires occurred mostly in the northern region (López Santalla & López García, 2019). One of these regions is Galicia. About 2/3 of the total surface area of this territory is classified as forest area and where more than half of the Spanish wood supply comes (Ministerio para la Transición Ecológica, 2021).

In this context, we propose a study to create a comprehensive and accurate dataset of forest fires, spanning a wide time frame, using an automatic, fast, and cost-effective procedure in terms of both monetary and technological aspects. Thus, allowing a rapid identification of forest fires (larger than 15 ha) for approximately the last 35 years, using multispectral satellite images from the free and public domain Landsat collection. The extensive temporal coverage of the Landsat mission makes it possible to cover periods of time not digitized in fire-related issues.

* Corresponding author

2. STUDY AREA

The study area is located in Northwest Spain, specifically in the community of Galicia (Figure 1) and covers all its provinces. It has a total of 313 municipalities, which 194 are classified as high-risk areas (ZAR) (Consellería do Medio Rural & Dirección Xeral de Defensa do Monte, 2022) in terms of forest fires.

The surface layers of the provinces, as well as the layers of the rivers and coast, are obtained from the Spanish Center for Geographical Information (CNIG) (Gobierno de España: Ministerio de Transportes, 2020).

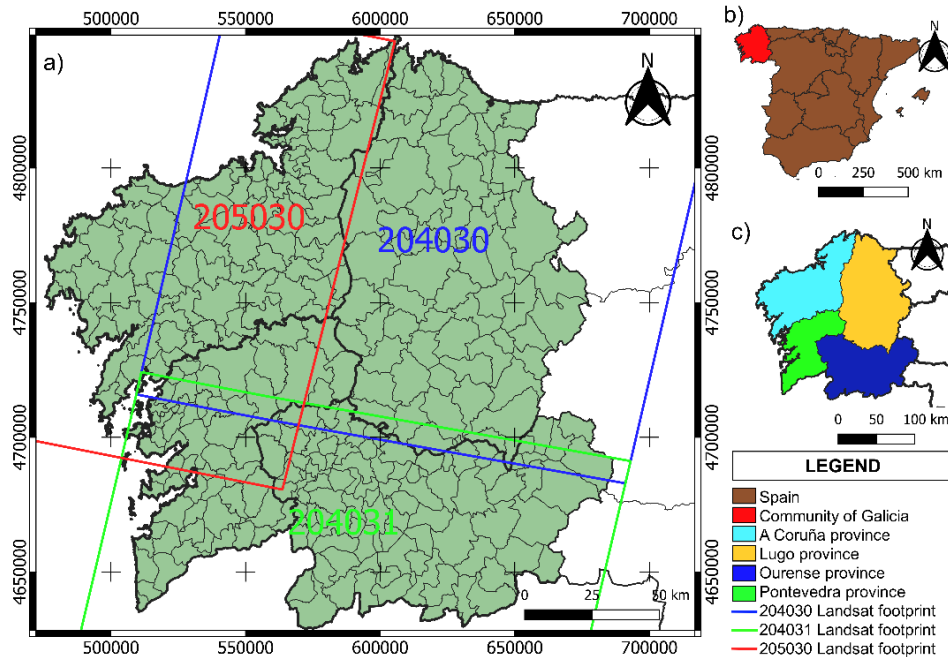


Figure 1. Location of the study area. a) Distribution of the municipalities and Landsat footprints in the Galician community (coordinate system EPSG: 25829). b) Location of Galicia in the Spanish territory. c) Location of provinces in Galician community.

3. METHODOLOGY

The overall methodology developed is illustrated in Figure 2 and consists of three phases: First, the acquisition and pre-processing of satellite images. Second, the processing of these satellite images. Finally, verification and visualization of the resulting layers.

The acquisition and pre-processing phase involves the generation of new images based on vegetation indices, using the "Normalized Difference Vegetation Index" (NDVI) or the "Normalized Burn Index" (NBR).

In the processing phase, layers or vector formats are created using the files obtained in the previous step. In this phase, a series of masks are obtained by reclassifying the vegetation index values or by performing unsupervised learning based on K-means clustering. The objective of this stage is to obtain the areas of disturbance from the NBR difference between two consecutive images and to apply the appropriate filters to ensure that these differences correspond to a fire disturbance in the forest land.

The final stage involves the verification and visualization of the resulting layers and their incorporation into a spatial database for future use.

3.1 Image Pre-processing and Download

3.1.1 Obtaining Images: Landsat satellite data are obtained and pre-processed using the Google Earth Engine (GEE) platform. The images used are those relating to the Footprint 204030, Footprint 204031, and Footprint 205030 of the Landsat-5 missions for the period 1985-2011 and Landsat-8 for the years 2013-2021. These satellite images belong to Collection 2 Level-2 Tier 1.

Therefore, the layers of the study area are uploaded to the GEE platform, which are used to upload the satellite image collection. A predefined GEE function is run to obtain the specific names of satellite images within this platform. In addition, a cloudiness filter is added to the collection.

After the names have been obtained for the respective dates, the corresponding satellite images are loaded into the GEE platform. Subsequently, they are scaled according to the United States Geological Survey (USGS).

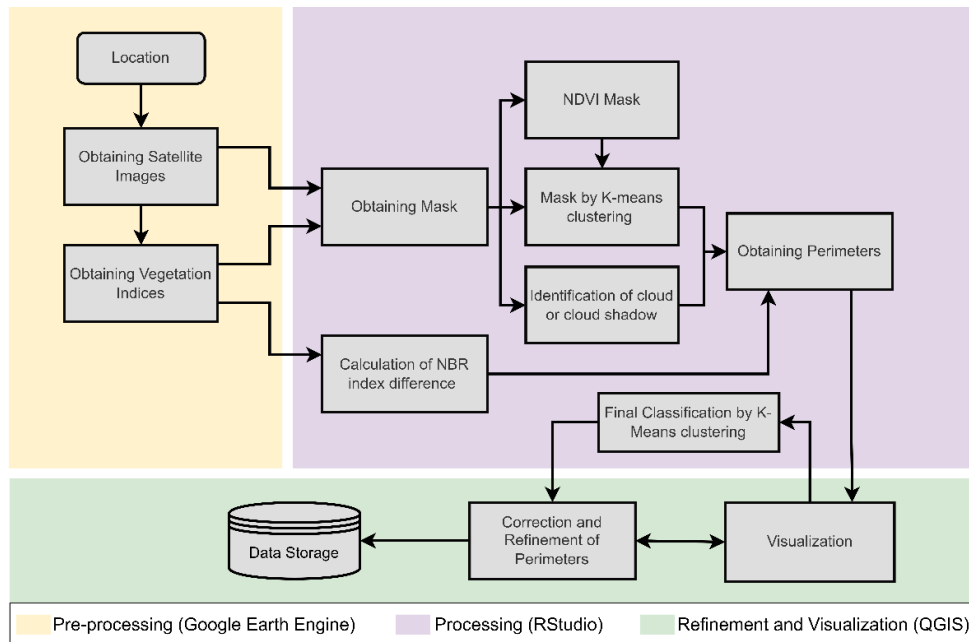


Figure 2. Workflow of the methodology

3.1.2 Obtaining Indices: After acquiring and scaling each Landsat image, the respective vegetation indices are calculated using GEE. A vegetation index is defined as the set of algebraic operations performed on the reflectance values at different wavelengths of the image pixels, which are sensitive to the vegetation cover (Gilbert et al., 1997), allowing the identification of certain characteristics.

Two vegetation indices are used. The first is the Normalized Difference Vegetation Index (NDVI) and the second is the Normalized Burn Ratio (NBR).

The NDVI provides an indication of the condition and health of vegetation by comparing the amount of visible red light absorbed and the amount of near infrared light reflected. The NDVI is calculated using Equation (1). Its results vary from -1 to 1, where negative values correspond to areas of high-water presence or artificial structures, bare natural soil usually ranges from 0.1 - 0.2, while plants are found in positive values ranging from 0.2 to 1.

$$NDVI = \frac{(NIR - RED)}{(NIR + RED)} \quad (1)$$

The NBR makes it possible to highlight burned areas and their severity after a fire. It corresponds to Equation (2). A high value usually corresponds to healthy vegetation, while low values usually indicate bare ground or burned surfaces.

$$NBR = \frac{(NIR - SWIR)}{(NIR + SWIR)} \quad (2)$$

3.1.3 Image Download: Both the previously calculated indices and a "stack" image consisting of the RGB bands (Red, Green and Blue) and the infrared bands (NIR, SWIR1 and SWIR2) are downloaded. In addition, another image is obtained with the "QA_PIXEL" band.

3.2 Image Processing

After the images have been downloaded, local processing in RStudio/2022.12.0 is developed to obtain perimeters through several masks. Three masks are obtained to filter out false positives. They are based on the NDVI index, unsupervised K-means clustering of reflectance values for the red band, and the band named "QA_PIXEL", which provides pixel quality attributes.

3.2.1 NDVI mask: The classification of vegetation presence or absence is based on NDVI values greater than 0.2. Pixel values are reclassified using this threshold, with values greater than 0.2 assigned a value of 1 and values less than or equal to 0.2 assigned a null value, resulting in a first binarized mask.

3.2.2 Grouping of The Red Band by K-Means: The following mask is based on the use of Machine Learning. The K-means algorithm is a type of unsupervised machine learning based on the clustering of object features into "k" groups. This clustering is done by optimizing the sum of the distances between each object and the centroid of its group.

The K-means algorithm is applied to the reflectance values of the red band (Landsat 5 = band 3 and Landsat 8 = band 4) to identify the location of forest structures from the satellite images. The red band allows the identification of different classes of vegetation because chlorophyll strongly absorbs light corresponding to the red part of the spectrum. It allows both greater contrast between areas with and without

vegetation and the identification of vegetation gradients (Delegido et al., 2011; Tucker, 1979). It makes it possible to separate the forest structures from agricultural areas.

To reduce the heterogeneity of reflectance values in the red band, the images are first masked using the previously obtained NDVI mask to only include only land with vegetation, before executing the clustering algorithm. A maximum of 500 iterations are used to generate 5 classes. An additional class is added. It contains null values as "-9999" to avoid affecting the grouping of other categories. The null values are subsequently removed.

The two clusters with the lowest reflectance value are identified as the possible groups to be forest and/or shrubland. In addition, the number of classes chosen is verified using the total within-cluster sum of squares or Elbow method.

3.2.3 "QA_PIXEL" Band Mask: The "QA_PIXEL" band is a quality control band used for Landsat images. It contains a decimal value for each pixel representing the combinations of fill bits for the surface, atmosphere, and sensor state conditions. The bits are assigned for distinguishable objects on the land surface with a wide range of confidence levels.

In order to use the pixel values in the quality control file, they must be transformed from decimal to 16-bit binary format. Single bits use 0 to indicate absence and 1 to indicate fulfilment. Double bits, such as 15-14, 13-12, 11-10, and 9-8, represent confidence level: 0 (none), 1 (low), 2 (medium), and 3 (high). All possible combinations of cloudiness and its derivatives are obtained, and at least one double bit must have a medium confidence level, except for 15-14. In addition, bits 0 and 2 are always set to 0.

After a smoothing filter is run to refine the images through the QGIS interface.

3.2.4 NBR Index Difference: The difference in NBR values (dNBR) between two images can be used to detect changes in the land surface. To calculate dNBR, the pre-fire NBR values are subtracted from the post-fire NBR values using Equation (3). The resulting set of pixel values indicates fire severity, with higher values indicating greater severity and lower values indicating regrowth after disturbance. The dNBR is reclassified according to severity levels, following Table 1.

$$dNBR = NBR_{prefire} - NBR_{postfire} \quad (3)$$

Severity	Level		
	dNBR Range	Normalized	
Regrowth, very high.	< -0.500	1	
Regrowth, high	-0.500 to -0.251	2	
Regrowth, low	-0.250 to -0.101	3	
Unburned	-0.100 to +0.99	4	
Low Severity	+0.100 to 0.269	5	
Moderate-low Severity	+0.270 to 0.399	6	
	+0.400 to 0.439	6.5	
Moderate-high severity	+0.440 to 0.479	7	
	+0.480 to 0.659	7.5	
High Severity	≥ 0.660	8	

Table 1. Normalization used for dNBR Range. Adapted from USGS.

3.2.5 Obtaining Perimeters: A combination of all previously obtained files is carried out to identify forest disturbance perimeters.

The normalized dNBR images are masked using the previously calculated files (as described in section 3.2.2 and section 3.2.3). A total of three layers of masks are applied, with two corresponding to the pre-fire image and one corresponding to the post-fire image. After three types of perimeters are obtained.

The first is the most restrictive perimeter. This perimeter makes it possible to obtain the starting point. It is extended to the rest of the pixels as long as the conditions for the area and the dNBR value are met. The starting condition is set for all values with an area greater than 0.5 ha with high severity (dNBR = 8) or values with an area greater than 12 ha but with moderate-high severity (dNBR = 7.5). The first case should be under the mask layer with the lowest reflectance, and the second case is under the two lower reflectance groups.

Therefore, the previous procedure of the first case is repeated (initial condition of dNBR = 8) but using the results of the K-means masking corresponding to the two lower reflectance groups. The two results of the first case are then intersected to increase the areas likely to be affected by wildfires. In both cases, an additional area of influence equivalent to 2 Landsat pixels is also used to identify the scattered pixels.

In addition, the overall area of each disturbance is obtained by setting a minimum value of 6.5 for dNBR and a minimum area of 15ha. The areas that meet both conditions are extracted. Lastly, the final disturbance perimeters are determined by intersecting the restrictive perimeters calculated above with the last results obtained for the overall area.

3.2.6 Final Classification of the Disturbance:

On the identified perimeters, a clustering based on K-means is again performed in order to obtain those areas that belong to forest fires.

The clustering is carried out using the NIR and SWIR1 bands. The K-means clustering algorithm is applied separately to each of these bands. Six classes are defined, one of which corresponds to null values (with a value of "-9999"). The modal value of the clustered pixels is then assigned to each polygon.

Burned areas typically have maximum reflectance values of up to 0.25 for the SWIR1 and up to 0.21-0.22 for the NIR (Ling et al., 2015). As a result, mean pixel clusters with reflectance values greater than 0.25 for the SWIR and 0.21 for the NIR are generally not indicative of burned areas. This range limitation is extended to the polygons, where any group inherited from the K-means process that exceeds the limit for NIR or SWIR is classified as a non-burned disturbance.

Finally, overlapping areas belonging to the same disturbance were identified and fixed. This overlap is due to individual identification of burned areas for each of the footprints in the common area between them.

4. RESULTS

This section shows some of the results of both the masks obtained and the perimeters of burned areas. As a general

result, a total of 12,687 perimeters of burned area greater than 15 ha were obtained for the 3 footprints studied, as shown in Table 2.

The following images (Figure 3, Figure 4, and Figure 5) show some of the results obtained for the time period from 2017/10/05 (as a pre-fires image) to 2017/11/06 (as a post-fires image). This is for the 204031 footprint.

The Figure 3 shows the set of masks obtained for the previous dNBR image. It shows the obtaining of the first mask (NDVI mask) as well as the two resulting masks belonging to K-means grouping. Figure 4 corresponds to the after image and shows the mask extracted for the purpose of filtering clouds and cloud shadows. Finally, Figure 5 is the result of the dNBR index, such as the extraction of the two limiting perimeters and the total area.

Footprint Name	Total Number of Burned Areas	
	(a)	(b)
204030	4,772	4,019
204031	5,324	5,127
205030	2,591	2,153

Table 2. Total perimeters identified. (a) with overlap. (b) with corrected overlap

Finally, as a general result of all the processed images and the elimination of the overlapping layers, the total perimeters obtained result in 11,299 affected areas (Table2), in which the areas with a recurrence of burned area were identified as

shown in Figure 6, being establishing up to a maximum value of greater than or equal to 3.

In addition, the results obtained were overlapped with historical data from the Spanish Ministry of Environment, which provides that information upon request. This data offers information on wildfires over long periods of time. However, the geographical location of forest fires is only given as a point on the land and covers the period from 1999 to 2015. To address this limitation, a buffer was created, and overlapping was carried out.

The results show that 73.68% of the burned areas obtained coincided with the Ministry data, while 40.83% of the total Ministry records could not be identified (as shown in Table 3). Moreover, if time periods without temporal continuity between images are excluded, such as the change from Landsat-5 to Landsat-8 in 2012 or the year 2002 when no image was available, the percentage of unidentified Ministry data decreases to 31.91%.

Footprint	Areas Obtained			Ministry Location	
	Total	Matches	%	Unidentified	%
204030	831	626	75.33	527	46.35
204031	1,578	1,146	72.62	727	39.48
205030	593	440	74.19	230	35.06
Total	3,002	2,212	73.68	1,484	40.83

Table 3. Overlap between the burned areas obtained and the Ministry of the Environment's forest fire records.

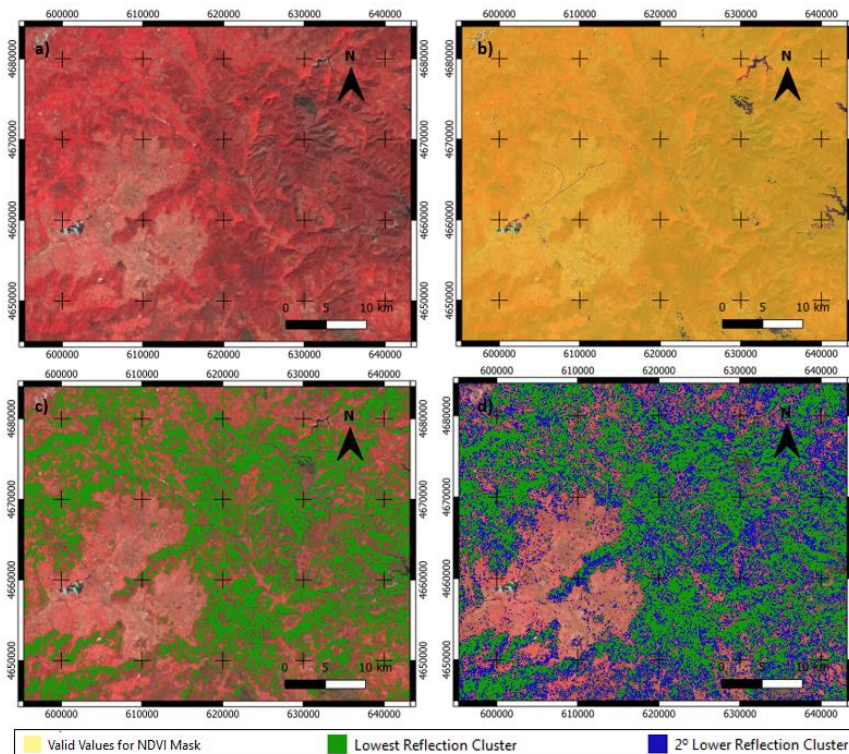


Figure 3. Pre-fires Image Layers. (a) Landsat Image in Infrared Composition. (b) NDVI Mask. (c) Lowest Reflectance Cluster Mask. (d) Mask of the Two Lowest Reflectance Clusters.

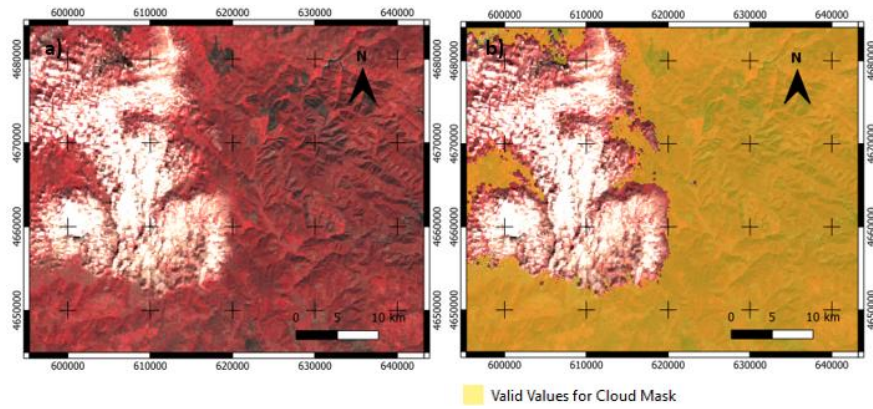


Figure 4. Post-fires Image Layer. (a) Landsat Image in Infrared Composition. (b) "QA_PIXEL" Band Mask.

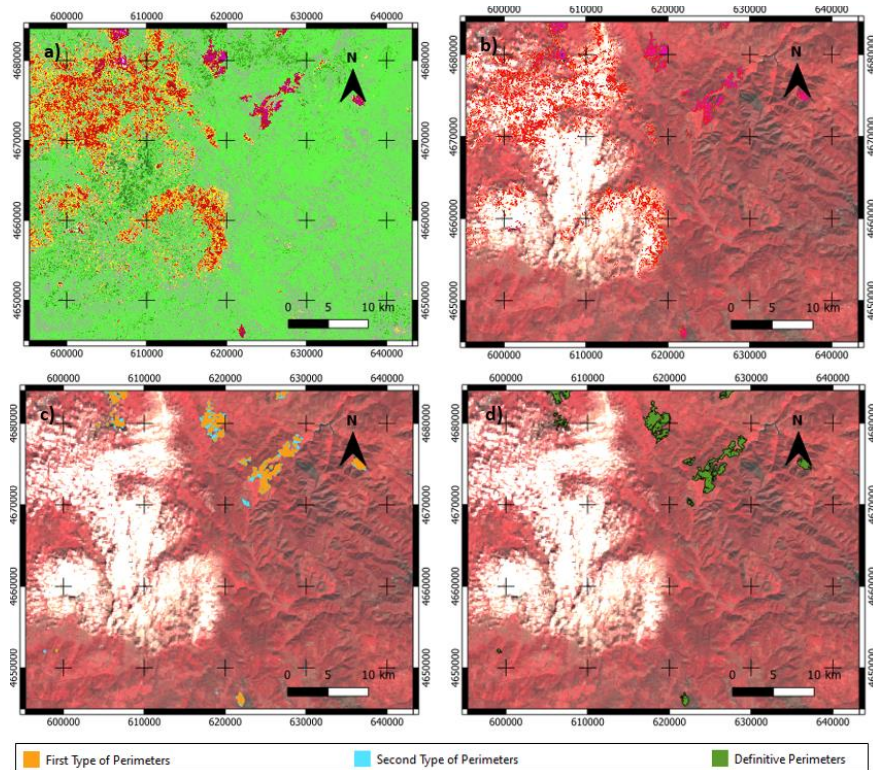


Figure 5. Resulting Layers. (a) dNBR Reclassified according to Severity Levels (Table 1). (b) dNBR Values meeting the Conditions (Section 3.2.5) (c) Limiting Perimeters. (d) Total Area of Perimeters.

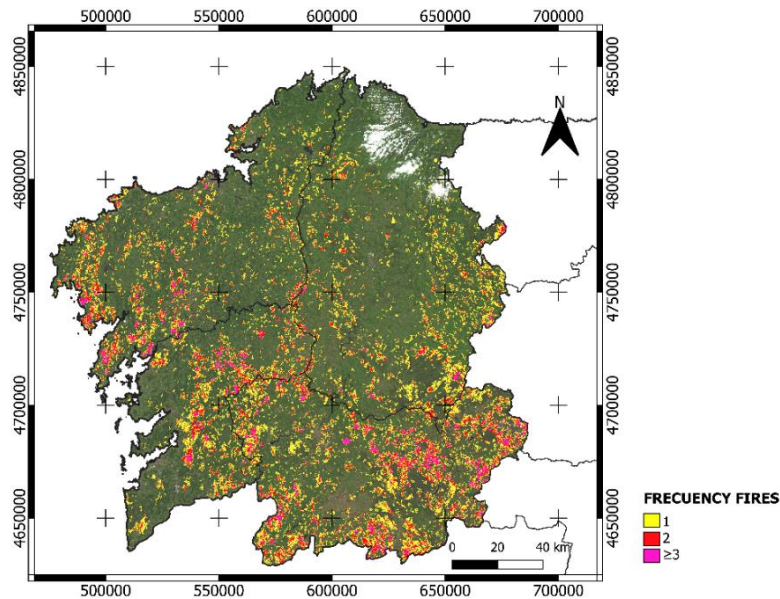


Figure 6. Location of burned area with its recurrence.

5. DISCUSSION

The use of satellite imagery for detecting burned areas by forest fires has become increasingly popular in recent years. This is due to its advantages of wide spatial coverage and the ability to obtain data frequently. In this paper, we proposed a novel method to obtain a real forest fire dataset during broad periods of time in an automated way. This approach, in contrast to other studies, without prior knowledge of the existence or location of disturbances on the ground.

All results were visually verified, identifying that in certain cases there were forest disturbances not identified in the records or forest fire points registered in lands not suitable for fire, such as urban areas or bodies of water. This may possibly be due to an error in the geolocation of official records, or the existence of prescribed burns not registered in official data as a fire but identified with this methodology.

Moreover, the possibility that not all fires that occurred during the analyzed period were identified is due to the limited availability of images in certain years. The unavailability of images due to several reasons, such as the change from Landsat-5 to Landsat-8 platform or certain sensor failures during image acquisition, results in long periods of time without image availability. This limitation reduces the ability to observe and delimit burned areas, as over time after the fire, the burned signal weakens due to vegetation recovery or ash removal (Melchiorre & Boschetti, 2018). This situation may cause some fires to go unnoticed.

Similarly, another important error is occlusion error, which is mainly caused by cloud cover that prevents the land surface from being seen in satellite images. Cloud cover can hinder the detection of burned areas and reduce the accuracy of their delineation, leading to errors in the dataset.

However, this methodology made it possible to obtain a dataset covering a broad time period, which allowed the heterogeneity of the data in terms of vegetation condition, land use, and image properties.

6. CONCLUSIONS

A methodology based on the automated processing of satellite images was developed to map forest fires larger than 15 hectares in Northwest Spain over the past 35 years. According to the results, 11,299 affected areas were identified.

The code was developed in R for image processing, which allowed to reduce mapping times and extra technological cost is practically null and typical of any digital user. Through the use of a personal computer (HP Intel Core - i7, 16Gb RAM, 1Tb SSD), we were able to process a large amount of satellite images of the last 35 years in order to delimit the burned areas.

Furthermore, the application of unsupervised learning based on K-Means clustering allowed us to quickly mask those areas not belonging to forest vegetation itself. The optimal number of classes for each image was obtained using Elbow method.

Obtaining and creating large datasets of forest fires is a suitable tool to build algorithms based on deep learning techniques for the automatic detection of these burned areas. To achieve this goal, data heterogeneity is essential. Future trends consist of the use of deep learning techniques that allow the automatic detection of historical burned areas.

ACKNOWLEDGEMENTS

This work was supported by “Ayudas para la Formación de Profesorado Universitario (FPU)”, Ministry of Education, Government of Spain [FPU21/03038]. We also acknowledge the funding by the European Union NextGenerationEU - Recovery and Resilience Mechanism (MRR/PRTR) through the grant TED2021-132000B-I00 of investment line I3.

REFERENCES

- Ban, Y., Zhang, P., Nascetti, A., Bevington, A. R., & Wulder, M. A. (2020). Near Real-Time Wildfire Progression Monitoring with Sentinel-1 SAR Time Series and Deep Learning. *Scientific Reports*, 10(1). <https://doi.org/10.1038/s41598-019-56967-x>

- Chuvieco, E., Mouillot, F., van der Werf, G. R., San Miguel, J., Tanasse, M., Koutsias, N., García, M., Yebra, M., Padilla, M., Gitas, I., Heil, A., Hawbaker, T. J., & Giglio, L. (2019). Historical background and current developments for mapping burned area from satellite Earth observation. *Remote Sensing of Environment*, 225, 45–64. <https://doi.org/10.1016/j.rse.2019.02.013>
- Cocke, A. E., Fulé, P. Z., & Crouse, J. E. (2005). Comparison of burn severity assessments using Differenced Normalized Burn Ratio and ground data. *International Journal of Wildland Fire*, 14(2), 189–198. <https://doi.org/10.1071/WF04010>
- Consellería do Medio Rural, & Dirección Xeral de Defensa do Monte. (2022). *PLADIGA 2022*.
- Das, S., & Angadi, D. P. (2022). Land use land cover change detection and monitoring of urban growth using remote sensing and GIS techniques: a micro-level study. *GeoJournal*, 87(3), 2101–2123. <https://doi.org/10.1007/s10708-020-10359-1>
- Delegido, J., Verrelst, J., Alonso, L., & Moreno, J. (2011). Evaluation of sentinel-2 red-edge bands for empirical estimation of green LAI and chlorophyll content. *Sensors*, 11(7), 7063–7081. <https://doi.org/10.3390/s110707063>
- Escuin, S., Navarro, R., & Fernández, P. (2008). Fire severity assessment by using NBR (Normalized Burn Ratio) and NDVI (Normalized Difference Vegetation Index) derived from LANDSAT TM/ETM images. *International Journal of Remote Sensing*, 29(4), 1053–1073. <https://doi.org/10.1080/01431160701281072>
- European Commission. (2022). *Forest Fires in Europe, Middle East and North Africa 2021*. JCR Technical Report.
- European Commission. (2021). *COMMUNICATION FROM THE COMMISSION TO THE EUROPEAN PARLIAMENT, THE COUNCIL, THE EUROPEAN ECONOMIC AND SOCIAL COMMITTEE AND THE COMMITTEE OF THE REGIONS - New EU Forest Strategy for 2030*.
- European Forest Fire Information System (EFFIS). (n.d.). Retrieved November 1, 2022, from <https://effis.jrc.ec.europa.eu/>
- Gilabert, M. A., González-Piqueras, J., & García-Haro, J. (1997). Acerca de los Índices de Vegetación. *Revista de Teledetección. Revista de La Asociación Española de Teledetección*, 8.
- Gobierno de España: Ministerio de Transportes, M. y A. Urbana. (2020). *Centro de Descargas del CNIG (IGN)*. DOI: 10.7419/162.09.2020. <http://centrodedescargas.cnig.es/CentroDescargas/index.jsp>
- Hawbaker, T. J., Vanderhoof, M. K., Schmidt, G. L., Beal, Y. J., Picotte, J. J., Takacs, J. D., Falgout, J. T., & Dwyer, J. L. (2020). The Landsat Burned Area algorithm and products for the conterminous United States. *Remote Sensing of Environment*, 244. <https://doi.org/10.1016/j.rse.2020.111801>
- Haynes, K., Short, K., Xanthopoulos, G., Viegas, D., Ribeiro, L. M., & Blanchi, R. (2020). Wildfires and WUI Fire Fatalities. In *Encyclopedia of Wildfires and Wildland-Urban Interface (WUI) Fires* (pp. 1–16). Springer International Publishing. https://doi.org/10.1007/978-3-319-51727-8_92-1
- Jactel, H., Branco, M., Duncker, P., Gardiner, B., Grodzki, W., Langstrom, B., Moreira, F., Netherer, S., Nicoll, B., Orazio, C., Piou, D., Schelhaas, M. J., & Tojic, K. (2012). A multicriteria risk analysis to evaluate impacts of forest management alternatives on forest health in Europe. *Ecology and Society*, 17(4). <https://doi.org/10.5751/ES-04897-170452>
- Jiao, L., & Bo, Y. (2022). Near real-time mapping of burned area by synergizing multiple satellites remote-sensing data. *GIScience & Remote Sensing*, 59(1), 1956–1977. <https://doi.org/10.1080/15481603.2022.2143690>
- Labenski, P., Ewald, M., Schmidlein, S., & Fassnacht, F. E. (2022). Classifying surface fuel types based on forest stand photographs and satellite time series using deep learning. *International Journal of Applied Earth Observation and Geoinformation*, 109, 102799. <https://doi.org/10.1016/j.jag.2022.102799>
- Ling, F., Du, Y., Zhang, Y., Li, X., & Xiao, F. (2015). Burned-Area Mapping at the Subpixel Scale with MODIS Images. *IEEE Geoscience and Remote Sensing Letters*, 12(9), 1963–1967. <https://doi.org/10.1109/LGRS.2015.2441135>
- Loboda, T. V., French, N. H. F., Hight-Harf, C., Jenkins, L., & Miller, M. E. (2013). Mapping fire extent and burn severity in Alaskan tussock tundra: An analysis of the spectral response of tundra vegetation to wildland fire. *Remote Sensing of Environment*, 134, 194–209. <https://doi.org/10.1016/j.rse.2013.03.003>
- López Santalla, A., & López García, M. (2019). *Decenio 2006-2015: Los Incendios Forestales en España*. Ministerio de Agricultura, Pesca y Alimentación - Secretaría General Técnica.
- Mallinis, G., Mitsopoulos, I., & Chrysafi, I. (2018). Evaluating and comparing sentinel 2A and landsat-8 operational land imager (OLI) spectral indices for estimating fire severity in a mediterranean pine ecosystem of Greece. *GIScience and Remote Sensing*, 55(1), 1–18. <https://doi.org/10.1080/15481603.2017.1354803>
- Melchiorre, A., & Boschetti, L. (2018). Global analysis of burned area persistence time with MODIS data. *Remote Sensing*, 10(5). <https://doi.org/10.3390/rs10050750>
- Ministerio para la Transición Ecológica. (2021). *Anuario de Estadística Forestal de España 2019*. www.miteco.es
- NASA EarthData Worldview . (n.d.). Retrieved November 1, 2022, from <https://www.earthdata.nasa.gov/worldview>
- Tucker, C. J. (1979). Red and Photographic Infrared linear Combinations for Monitoring Vegetation. In *REMOTE SENSING OF ENVIRONMENT* (Vol. 8).
- Yang, Q., Liu, X., Huang, Z., Guo, B., Tian, L., Wei, C., Meng, Y., & Zhang, Y. (2022). Integrating satellite-based passive microwave and optically sensed observations to evaluating the spatio-temporal dynamics of vegetation health in the red soil regions of southern China. *GIScience and Remote Sensing*, 59(1), 215–233. <https://doi.org/10.1080/15481603.2021.2023841>